

AD-A054 934

NAVAL RESEARCH LAB WASHINGTON D C
EFFECTS OF COLLISIONS ON LEVEL POPULATIONS AND DIELECTRONIC REC--ETC(U)
APR 78 V L JACOBS, J DAVIS

F/G 20/9

NASA-DPR-60404-G

UNCLASSIFIED

NRL-MR-3641

NL

| OF |
AD
A054934



AD A 054934

AD No. _____
DDC FILE COPY

12
b.s.

FOR FURTHER TRAN

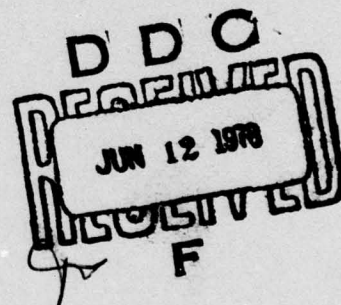
NRL Memorandum Report 3641

Effects of Collisions on Level Populations and Dielectronic Recombination Rates of Multiply-Charged Ions

V. L. JACOBS AND J. DAVIS

Plasma Physics Division

April 1978



NAVAL RESEARCH LABORATORY
Washington, D.C.

Approved for public release: distribution unlimited.

SECURITY CLASSIFICATION OF THIS PAGE (When Data Entered)

REPORT DOCUMENTATION PAGE		READ INSTRUCTIONS BEFORE COMPLETING FORM
1. REPORT NUMBER NRL Memorandum Report 3641	2. GOVT ACCESSION NO.	3. RECIPIENT'S CATALOG NUMBER
4. TITLE (and Subtitle) EFFECTS OF COLLISIONS ON LEVEL POPULATIONS AND DIELECTRONIC RECOMBINATION RATES OF MULTIPLY-CHARGED IONS		5. TYPE OF REPORT & PERIOD COVERED Interim report on a continuing NRL project
6. AUTHOR(s) V. L. Jacobs - J. Davis		7. PERFORMING ORG. REPORT NUMBER
8. PERFORMING ORGANIZATION NAME AND ADDRESS Naval Research Laboratory Washington, D. C. 20375		9. CONTRACT OR GRANT NUMBER(s) NASA-DPR-60404-G
10. CONTROLLING OFFICE NAME AND ADDRESS National Aeronautics and Space Administration Washington, D. C. 20545		11. PROGRAM ELEMENT, PROJECT, TASK AREA & WORK UNIT NUMBERS NRL Problem No. 77H02-24 NASA Grant No. DPR-60404-G
12. MONITORING AGENCY NAME & ADDRESS (if different from Controlling Office)		13. REPORT DATE Apr 78
14. SECURITY CLASS. (of this report) UNCLASSIFIED		15. NUMBER OF PAGES 41
16. DISTRIBUTION STATEMENT (of this Report) Approved for public release; distribution unlimited.		17. DECLASSIFICATION/DOWNGRADING SCHEDULE
18. DISTRIBUTION STATEMENT (of the abstract entered in Block 20, if different from Report) NRL-MR-3641		
19. SUPPLEMENTARY NOTES		
20. KEY WORDS (Continue on reverse side if necessary and identify by block number) Dielectronic Recombination Ionization Equilibrium Atomic Processes in Plasmas Autoionization		
21. ABSTRACT (Continue on reverse side if necessary and identify by block number) A generalization of previously reported statistical theories is developed for determining the excited level populations and the ionization-recombination balance of multiply-charged atomic ions in an optically-thin high-temperature plasma. Account is taken of the most important collisional and radiative processes involving bound and autoionizing levels in three consecutive ionization stages. We obtain a set of rate equations for the population densities of the low-lying levels which contains effective excitation, ionization, and recombination rates describing		

DDC
JUN 12 1978
F

DD FORM 1 JAN 73 1473

EDITION OF 1 NOV 65 IS OBSOLETE
S/N 0102-LF-014-6601

SECURITY CLASSIFICATION OF THIS PAGE (When Data Entered)

251 950

self

20. Abstract (Cont'd)

indirect transitions through the more highly-excited bound and autoionizing levels. The familiar corona model equations for the ground state populations are recovered by making the assumption that all excited states decay by only spontaneous radiative or autoionization processes. When collisional processes become efficient in depopulating the highly-excited levels important in dielectronic recombination, the effective rate of recombination must be described by a collisional-dielectronic recombination coefficient. Results of calculations are presented for the collisional-dielectronic recombination rate coefficients for recombination of Fe^{+8} - Fe^{+13} ions. At an electron density of 10^{16} cm^{-3} , dielectronic recombination is still the dominant recombination process. However, the collisional-dielectronic recombination rate coefficients are found to be reduced by about an order of magnitude from their corona model values due to the effects of multiple collisional excitations on the populations of the highly-excited bound levels of the combined ion. The dielectronic recombination rates into these highly-excited levels are found to be enhanced by the effects of collisionally induced angular momentum redistribution on the populations of the autoionizing levels.

CONTENTS

I. INTRODUCTION	1
II. INDIVIDUAL COLLISIONAL AND RADIATIVE PROCESSES	5
III. EFFECTIVE TRANSITION RATES	9
IV. CALCULATIONS	19
V. CONCLUSIONS	28
ACKNOWLEDGMENTS	29
REFERENCES	29

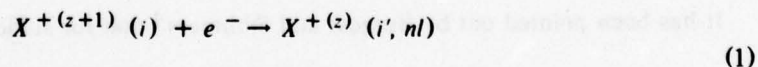
ACCESSION FOR	
NTIS	WPA Section <input checked="" type="checkbox"/>
DDI	D.I. Section <input type="checkbox"/>
HANDLING D	
J. G. T. 101	
BY	
DISTRIBUTION/AVAILABILITY CODES	
D: / or SPECIAL	
A	

EFFECTS OF COLLISIONS ON LEVELS POPULATIONS AND DIELECTRONIC RECOMBINATION RATES OF MULTIPLY CHARGED IONS

I. INTRODUCTION

The physical properties of high-temperature laboratory and astrophysical plasmas can be deduced from an analysis of optically-thin spectral line intensities emitted by multiply-charged atomic ions undergoing transitions between low-lying bound levels.^{1,2} The theoretical prediction of the spectral line intensities is complicated by the fact that the low-lying levels can be significantly populated by cascade transitions from the more highly-excited levels. In the solar corona and in low-density laboratory plasmas such as tokamak discharges, incompletely-stripped ions can recombine predominantly by means of the dielectronic recombination process described by Burgess³, in which highly-excited bound and autoionizing levels can play the most important role. In this investigation, a consistent statistical description is given of the contributions from highly-excited bound and autoionizing levels to effective excitation, ionization, and recombination rates between low-lying bound levels. Calculations are presented for recombination rates for which these contributions are expected to be most important.

The dielectronic recombination process described by Burgess³ is initiated with the formation of a doubly-excited autoionizing state through a radiationless capture



of an electron into a state nl accompanied by the excitation $i \rightarrow i'$ of one of the bound electrons in the recombining ion. The initial state i of the $(z+1)$ -times ionized ion $X^{+(z+1)}$ is

Manscript submitted October 7, 1977.

usually the ground state i_0 , but recombination from a metastable state may also be important. Recombination is accomplished when the doubly-excited state undergoes a stabilizing radiative transition

$$X^{+(z)}(i', nl) \rightarrow X^{+(z)}(i_0, nl) + \hbar \omega \quad (2)$$

to a singly-excited state below the ionization threshold.

At sufficiently low densities all stabilizing radiative transitions (2) will be followed by cascade transitions

$$X^{+(z)}(i_0, nl) \rightarrow X^{+(z)}(i_0, n'' l'') + \hbar \omega'' \quad (3)$$

which will eventually terminate in the ground state $j_0 = i_0, n_0 l_0$ or a metastable state of the recombined ion. The total recombination rate to the ground state is then given simply by

$$R_d(i \rightarrow j_0) = \sum_{i', nl} A_r(i', nl \rightarrow i_0, nl) N(i', nl), \quad (4)$$

where $A_r(i', nl \rightarrow i_0, nl)$ denotes the spontaneous radiative decay rate for the stabilizing transition (2). The doubly-excited level population densities $N(i', nl)$ are given by

$$N(i', nl) = \frac{N(i) N_e C_{cap}(i \rightarrow i', nl)}{A_a(i', nl) + A_r(i', nl)}, \quad (5)$$

where $C_{cap}(i \rightarrow i', nl)$ is the rate coefficient for the radiationless capture (1) and the total decay rates due to all spontaneous radiative and autoionization processes are denoted by $A_r(i', nl)$ and $A_a(i', nl)$, respectively. N_e and $N(i)$ are the electron and the initial ion densities, respectively.

It has been pointed out by Burgess and Summers⁴ that for sufficiently high electron densities the most important singly-excited levels will be significantly depopulated by the collisional excitation and ionization processes

$$X^{+(z)}(i_o, nl) + e^- \rightarrow X^{+(z)}(i_o, n'l') + e^- \quad (6)$$

and

$$X^{+(z)}(i_o, nl) + e^- \rightarrow X^{+(z+1)}(i_o) + e^- + e^-. \quad (7)$$

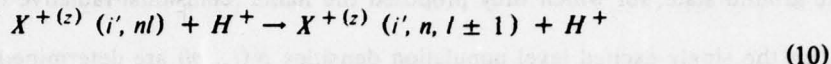
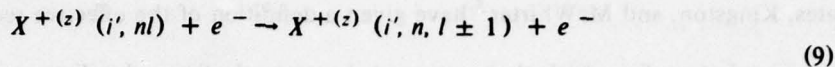
Bates, Kingston, and McWhirter⁵ have given a definition of the effective recombination rate to the ground state, for which they proposed the name "collisional-radiative recombination rate", when the singly-excited level population densities $N(i_o, nl)$ are determined by both collisional and radiative processes. However, dielectronic recombination was not taken into account in their investigation. Burgess and Summers⁴ proposed the name "collisional-dielectronic recombination rate" for the effective recombination rate obtained with the inclusion of dielectronic recombination. The collisional-dielectronic recombination rate is given, in terms of the total collisional-radiative transition rates

$$R_{cd}(i \rightarrow j_o) = \sum_{nl} W(i_o, nl \rightarrow i_o, n_o l_o) N(i_o, nl). \quad (8)$$

The collisional processes (6) and (7) together with their inverses tend to bring the singly-excited level population densities $N(i_o, nl)$ closer to their Boltzmann-Saha equilibrium values, which are found to be much smaller than predicted when only radiative and dielectronic recombination and cascade transitions are taken into account. Therefore, collisional processes tend to reduce the effective recombination rate. Since the most important $\Delta n \neq 0$ collisional processes are found to be associated with the $n' = n \pm 1$ transitions, the reduction may be said to be accomplished through multiple collisional excitations to more highly-excited levels from which ionization is more probable.

Electron- and proton-induced transitions corresponding to $n' = n$ and $l' = l \pm 1$ are known to be the most rapid collisional processes involving the multiply charged ions in a

predominantly hydrogen plasma. Burgess and Summers⁴ made the assumption that these processes are rapid enough to establish a Boltzmann distribution with respect to l for all values of n . They also pointed out that the corresponding angular momentum redistribution processes involving doubly-excited states



would produce an enhancement of the dielectronic recombination rate into the sublevels associated with a given value of n , but this effect was neglected in their calculations. Independent calculations by Jacobs, Davis, and Kepple⁶ and by Seaton and Storey⁷ have now established that collisionally-induced angular momentum redistribution of the doubly-excited level populations can amplify the dielectronic recombination rates into the highly-excited levels. The calculations of the collisional-dielectronic recombination rates reported in this paper are, to the best of our knowledge, the first in which explicit account is taken of the rates for collisionally-induced angular momentum mixing of both the singly- and the doubly-excited states.

A detailed discussion is given in section II of the individual collisional and radiative processes which are taken into account in the present investigation. In section III a set of rate equations for the population densities of the low-lying levels is derived which contains effective transition rates describing indirect transitions through the more highly-excited bound and autoionizing levels. By taking into account processes involving bound and autoionizing states in three consecutive ionization stages, we obtain a generalization of previously reported statistical theories.^{4,5,8} Certain aspects of the general theory are illustrated in section IV, where calculations are described for the collisional-dielectronic recombination rate coefficients for recombination of $Fe^{+8} - Fe^{+13}$ ions. Our conclusions are given in section V.

II. INDIVIDUAL COLLISIONAL AND RADIATIVE PROCESSES

In this section we discuss the individual collisional and radiative processes which are expected to be most important in determining the level populations of multiply-charged ions. In some cases we introduce total transition rates or rate coefficients between levels which include the contributions from both collisional and radiative processes. Since we will ignore collisions between the multiply-charged ions, we shall assume that they are present in sufficiently small concentrations in a predominantly hydrogen plasma. Since only spontaneous radiative processes will be taken into account in the present investigation, we shall also assume that the plasma is optically-thin to its own emitted radiation and that no external radiation fields are present. However, we will indicate which of the total transition rates and rate coefficients can be influenced by contributions from processes induced by a radiation field.

In the present investigation, we will take into account only transitions between levels within an ionization stage and those connecting adjacent ionization stages. Double ionization processes, for example, will be neglected. To simplify the notation used in the following section, we will adopt the convention of denoting bound states of the three consecutive ions $X^{+(z+1)}$, $X^{+(z)}$, and $X^{+(z-1)}$ by the indices i , j , and k , respectively. Autoionizing states of the ions $X^{+(z)}$ and $X^{+(z-1)}$ will be denoted by a and b , respectively. Different states belonging to the same stage of ionization will be distinguished by using, for example, j , j' , and \bar{j} . In this investigation the singly-excited bound states will be specified by $j = i_0, nl$, where i_0 is the ground state of the ion $X^{+(z+1)}$. The corresponding doubly-excited autoionizing states will be specified by $a = i', nl$, where i' is an excited state.

The total collisional-radiative transition rate connecting the bound states j and j' , which are in the same ionization stage, is given by

$$W(j, j') = A_r(j' \rightarrow j) \theta(E_{j'} - E_j) + N_e C_e(j' \rightarrow j) + N_{H^+} C_{H^+}(j' \rightarrow j). \quad (11)$$

The rate for the spontaneous radiative decay process

$$X^{+(z)}(j') \rightarrow X^{+(z)}(j) + \hbar\omega \quad (12)$$

is denoted by $A_r(j' \rightarrow j)$, and the θ function is used to insure that emission terms contribute only when $E_j < E_{j'}$. The corresponding stimulated emission and photo-excitation rates must be included when the interaction with a radiation field is investigated. The rate coefficients describing the collisional processes

$$X^{+(z)}(j') + e^- \rightarrow X^{+(z)}(j) + e^- \quad (13)$$

and

$$X^{+(z)}(j') + H^+ \rightarrow X^{+(z)}(j) + H^+, \quad (14)$$

which are denoted by $C_e(j' \rightarrow j)$ and $C_{H^+}(j' \rightarrow j)$, are functions of the local temperatures T_e and T_{H^+} . The electron and proton densities are denoted by N_e and N_{H^+} . Electrons are known to be more efficient in causing transitions corresponding to energy differences comparable with $k_B T_e$, while protons become more important for transitions between the nearly-degenerate l -sublevels corresponding to large n -values. With increasing n , radiative decay becomes less probable, whereas collisional transitions between neighboring levels occur more rapidly.

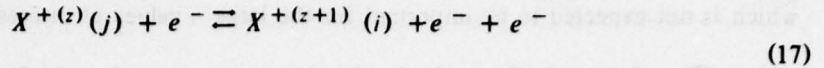
The bound-free and total free-bound rate coefficients

$$S(i, j) = S_e(j \rightarrow i) \quad (15)$$

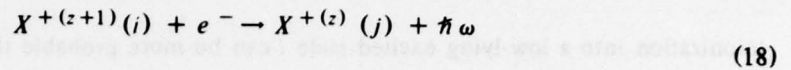
and

$$\alpha(j, i) = \alpha_r(i \rightarrow j) + N_e \alpha_3(i \rightarrow j) \quad (16)$$

describe direct transitions between the bound states i and j , which are in adjacent stages of ionization. The rate coefficients for the electron impact ionization and three-body recombination processes

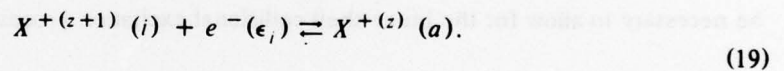


are denoted by $S_e(j \rightarrow i)$ and $\alpha_3(i \rightarrow j)$, respectively. Charge exchange processes are neglected in the present investigation. The rate coefficient describing the spontaneous radiative recombination process



is denoted by $\alpha_r(i \rightarrow j)$. To investigate the interaction with a radiation field, $S(i, j)$ must include a term describing photoionization, while the stimulated radiative recombination rate coefficient must be included in $\alpha(j, i)$. The direct ionization and radiative recombination processes result predominantly in the production of relatively low-lying states. Three-body recombination becomes more important than direct radiative recombination with increasing n and N_e , but dielectronic recombination is more often the dominant recombination process at low and intermediate densities.

We will assume that transitions between the autoionizing state a and the adjacent continuum state i, ϵ_i occur only by means of the radiationless capture and inverse autoionization processes



The capture coefficient and the autoionization rate will be denoted, respectively, by

$$C_{cap}(a, i) = C_{cap}(i \rightarrow a) \quad (20)$$

and

$$A_a(i, a) = A_a(a \rightarrow i). \quad (21)$$

We will neglect the corresponding three-body capture and collisional ionization processes described by Weisheit⁹, which may become important only at very high densities or for very large n . We will also neglect the spontaneous radiative Auger process described by Åberg¹⁰,

which is not expected to be important for the large n values of interest in the present investigation. The photoexcitation and stimulated emission processes which can occur between these states will be systematically treated in a subsequent investigation. Although the rate for radiationless capture into the doubly-excited state $a = i'$, $n!$ decreases as n^{-3} , the dominant contributions to the dielectronic recombination rate are often associated with large values of n . Autoionization into a low-lying excited state i can be more probable than autoionization into the ground state i_0 . The inclusion of this additional autoionization process has been found¹¹ to result in a substantial reduction in the dielectronic recombination rates for certain ionization states.

The stabilizing transition from the autoionizing state a to the state j , below the ionization threshold, will be assumed to occur only by means of the spontaneous radiative decay process

$$X^{+(z)}(a) \rightarrow X^{+(z)}(j) + \hbar\omega \quad (22)$$

with a rate denoted by

$$A_r(j, a) = A_r(a \rightarrow j). \quad (23)$$

In order to obtain the contributions from autoionizing states to effective ionization rates, it will be necessary to allow for the inner-shell collisional excitation process

$$X^{+(z)}(j) + e^- \rightarrow X^{+(z)}(a) + e^- \quad (24)$$

described by the rate coefficient

$$C_e(a, j) = C_e(j \rightarrow a). \quad (25)$$

It has been argued by Bates and Dalgarno¹² and by Burgess and Summers⁴ that the collisional stabilization rate associated with the inverse of the excitation process (24) can become comparable with the spontaneous radiative decay rate only at very high densities, because the inner-shell de-excitation process involves relatively low-lying levels. It is also apparent for the same

reason that the corresponding stimulated radiative decay and inner-shell photoexcitation process will become important only in the presence of intense radiation fields at relatively short wavelengths. These additional processes will be treated in a future investigation.

The total collisional-radiative transition rate $W(a, a')$ between autoionizing states of the z -times ionized ion is defined by an expression which is analogous to equation (11).

The autoionizing resonances and the adjacent continua can be treated as separate states provided that the resonance level separations are large compared with their total widths, which are determined by all spontaneous autoionization and radiative decay processes. An analysis by Seaton¹³ indicates that this treatment becomes a better approximation with increasing z provided that the radiative decay width can be neglected. Shore¹⁴ has shown that overlapping resonances with different angular momentum quantum numbers can still be treated as separate states.

III. EFFECTIVE TRANSITION RATES

In this section we combine and generalize previously reported statistical theories^{4,5,8} in order to derive a set of rate (time-dependent) equations for the population densities of the low-lying levels which contains effective transition rates describing indirect transitions through the more highly-excited bound and autoionizing levels. The number of low-lying levels which are to be explicitly included in these rate equations will depend on the problem of interest. Bates, Kingston, and McWhirter⁵ allowed for the time dependences of only the ground state population densities and introduced definitions of the effective recombination and ionization rates through the bound excited states. Burgess and Summers⁴ extended these definitions by including dielectronic recombination into the excited levels in addition to direct radiative and three-body recombination, but transitions between autoionizing levels were neglected. In a recent investigation⁸, Burgess and Summers defined generalized effective transition rates

between a group of low-lying levels, which have relatively long relaxation times; but processes involving autoionizing states were neglected.

The rate equations obtained in previous investigations describe transitions between levels in only two adjacent ionization stages. By taking into account transitions involving bound and autoionizing levels in three consecutive ionization stages, we are able to derive a more general set of rate equations for the low-lying level populations which contains three different generalized effective transition rates. The familiar corona model equations for the ground state population densities will be recovered by making the assumption that all excited states decay by only spontaneous radiative or autoionization processes. At densities for which only the highly-excited levels important in dielectronic recombination are appreciably depopulated by collisional processes, the ionization rate remains essentially unaltered but the effective rate of recombination must be described by a collisional-dielectronic recombination rate coefficient.

Using the notation introduced in the preceding section for the various transition rates and rate coefficients, the rate equations satisfied by the bound level population densities $N(j)$ of the z -times ionized ion can be written in the form

$$\begin{aligned} \frac{dN(j)}{dt} = & - \sum_{j'} Q(j, j') N(j') \\ & + \sum_i \alpha(j, i) N(i) N_e + \sum_k S(j, k) N(k) N_e \\ & + \sum_a A_r(j, a) N(a) + \sum_b A_a(j, b) N(b), \end{aligned} \quad (26)$$

where

$$Q(j, j') = -W(j, j') \text{ for } j \neq j' \quad (27)$$

and

$$Q(j, j) = \sum_{j' \neq j} W(j', j) + N_e \left[\sum_i S(i, j) + \sum_k \alpha(k, j) + \sum_a C_e(a, j) + \sum_b C_{cap}(b, j) \right]. \quad (28)$$

Equation (26) describes the population of the bound state j due to bound-bound transitions, direct recombinations, direct ionizations, stabilizing radiative transitions, and autoionization processes. Equation (28) gives the total depopulation rate $Q(j, j)$ which results from bound-bound transitions, direct ionizations, direct recombinations, inner-shell collisional excitations, and radiationless captures. The transitions, involving bound and autoionizing states in the three consecutive ionization stages, which are taken into account in the determination of $N(j)$ are illustrated by the vertical lines in Figure 1. The rates or rate coefficients associated with the various excitation and de-excitation processes are also indicated. Neutral atoms and completely-stripped ions clearly represent special cases for which only two adjacent ionization stages are involved.

The autoionizing level population densities $N(a)$ of the z -times ionized ion satisfy the rate equations

$$\begin{aligned} \frac{dN(a)}{dt} = & - \sum_{a'} Q(a, a') N(a') \\ & + \left[\sum_i C_{cap}(a, i) N(i) + \sum_j C_e(a, j) N(j) \right] N_e, \end{aligned} \quad (29)$$

where

$$Q(a, a') = -W(a, a') \text{ for } a \neq a' \quad (30)$$

and

$$Q(a, a) = \sum_{a' \neq a} W(a', a) + \sum_i A_a(i, a) + \sum_j A_r(j, a). \quad (31)$$

Equation (29) describes the population of the autoionizing level a due to transitions from nearby autoionizing levels, radiationless captures, and inner-shell collisional excitations. $Q(a, a)$ is the total depopulation rate arising from transitions to nearby autoionizing levels, autoionization processes, and stabilizing radiative transitions.

Following the procedure of Bates, Kingston, and McWhirter⁵, we shall retain the time derivatives for only a group of low-lying bound levels, consisting of the ground level and a certain number of metastable levels, which we shall denote by, for example, j and j' . The more highly-excited bound levels, which will be denoted by \bar{j} and \bar{j}' , will be assumed to have their steady-state (statistical equilibrium) population densities. It is usually assumed that ionization and recombination processes occur predominantly from the low-lying bound levels, because the highly-excited level populations are negligible in comparison. However, in order to obtain the collisional-dielectronic recombination coefficients associated with recombination from the z -times ionized ion, it will be necessary to allow for ionization from the highly-excited bound states \bar{k} produced by dielectronic recombination.

The statistical equilibrium population densities $N(\bar{j})_{eq}$ of the highly-excited bound levels \bar{j} are given, in terms of the population densities of the low-lying bound levels i, j , and k and the autoionizing levels a and b , by

$$\begin{aligned}
 N(\bar{j})_{eq} = & - \sum_{\bar{j}'} \sum_j \bar{Q}^{-1}(\bar{j}, \bar{j}') Q(\bar{j}', j) N(j) \\
 & + \sum_{\bar{j}'} \sum_i \bar{Q}^{-1}(\bar{j}, \bar{j}') \alpha(\bar{j}', i) N(i) N_e \\
 & + \sum_{\bar{j}'} \sum_k \bar{Q}^{-1}(\bar{j}, \bar{j}') S(\bar{j}', k) N(k) N_e \\
 & + \sum_{\bar{j}'} \sum_a \bar{Q}^{-1}(\bar{j}, \bar{j}') A_r(\bar{j}', a) N(a) \\
 & + \sum_{\bar{j}'} \sum_b \bar{Q}^{-1}(\bar{j}, \bar{j}') A_a(\bar{j}', b) N(b).
 \end{aligned} \tag{32}$$

In the next section we will describe the techniques which must be used to invert the rather large matrix \bar{Q} , which is defined within the subspace of the highly-excited bound levels \bar{j} . Analogous expressions are obtained for $N(\bar{i})_{eq}$ and $N(\bar{k})_{eq}$.

We will assume that all autoionizing levels a have their statistical equilibrium population densities $N(a)_{eq}$ given by

$$\begin{aligned} N(a)_{eq} = & \sum_{a'} \sum_i Q^{-1}(a, a') C_{cap}(a', i) N(i) N_e \\ & + \sum_{a'} \sum_j Q^{-1}(a, a') C_e(a', j) N(j) N_e. \end{aligned} \quad (33)$$

When transitions between the autoionizing levels are neglected, the first term on the right hand side reduces to the usual result for the population densities of the doubly-excited levels formed by radiationless capture. The second term, which gives the contributions from inner-shell collisional excitations, is important only for relatively small values of the outer electron principal quantum number n . An analogous expression is obtained for $N(b)_{eq}$ in terms of the population densities $N(j)$ and $N(k)$.

After expressing the population densities of the more highly-excited bound and autoionizing levels in terms of the population densities of the low-lying levels in three consecutive ionization stages, we obtain a reduced set of rate equation which can be written in the form

$$\begin{aligned} \frac{dN(j)}{dt} = & - \sum_{j'} Q_{eff}(j, j') N(j') \\ & + \sum_i \alpha_{eff}(j, i) N(i) N_e \\ & + \sum_k S_{eff}(j, k) N(k) N_e. \end{aligned} \quad (34)$$

The three effective transition rates which appear in these equations are rather small matrices which are defined only within the subspace of the low-lying levels explicitly included.

The matrix elements $Q_{eff}(j, j')$ with $j \neq j'$ are the effective bound-bound transition rates between the low-lying levels of the ion $X^{+(z)}$, while the diagonal elements $Q_{eff}(j, j)$ represent the total effective loss rates from these levels. The general expression obtained for $Q_{eff}(j, j')$ can be written in the form

$$\begin{aligned} Q_{eff}(j, j') &= Q_T(j, j') - \sum_j \sum_{\bar{j}} Q(j, \bar{j}) \bar{Q}^{-1}(\bar{j}, \bar{j}') Q_T(\bar{j}', j') \\ &- \sum_k \sum_{\bar{k}'} N_e S(j, \bar{k}) \bar{Q}^{-1}(\bar{k}, \bar{k}') N_e \alpha_T(\bar{k}', j') \\ &- \sum_i \sum_{\bar{i}'} N_e \alpha(j, \bar{i}) \bar{Q}^{-1}(\bar{i}, \bar{i}') N_e S_T(\bar{i}', j'), \end{aligned} \quad (35)$$

where

$$\begin{aligned} Q_T(j, j') &= Q(j, j') - \sum_a \sum_{a'} A_r(j, a) Q^{-1}(a, a') N_e C_e(a', j') \\ &- \sum_b \sum_{b'} A_a(j, b) Q^{-1}(b, b') N_e C_{cap}(b', j'). \end{aligned} \quad (36)$$

and the corresponding definitions of $\alpha_T(k, j)$ and $S_T(i, j)$ are given by expressions which are analogous to equations (38) and (40).

The total transition rate $Q_T(j, j')$ is obtained as the sum of the direct term $Q(j, j')$ and two additional contributions describing indirect transitions through the autoionizing levels a and b in two adjacent ionization stages. The third term in equation (36), which describes autoionization following radiationless capture, reduces to the result obtained by Seaton¹³ when transitions between the autoionizing levels b are neglected. The second term, which represents stabilizing radiative transitions of autoionizing levels a formed by inner-shell collisional excitation, has not been discussed previously.

The general expression for $Q_{eff}(j, j')$, which includes the contributions from indirect transitions through the highly-excited bound levels in three consecutive ionization stages, becomes equivalent to the definition given in the recent paper by Burgess and Summers⁸ when only the direct transition rate $Q(j, j')$ is included in $Q_T(j, j')$ and the last two of the three double summations are omitted. The last double summation, which describes recombination following ionization, is not expected to be important for highly-excited states \bar{i} . However, the preceding double summation, which describes ionization from highly-excited states \bar{k} populated by recombination, will be important.

The general expression obtained for the effective recombination coefficient $\alpha_{eff}(j, i)$ can be written in the form

$$\begin{aligned} \alpha_{eff}(j, i) = & \alpha_T(j, i) - \sum_j \sum_{\bar{j}} Q(j, \bar{j}) \bar{Q}^{-1}(\bar{j}, \bar{j}') \alpha_T(\bar{j}', i) \\ & - \sum_i \sum_{\bar{i}} \alpha(j, \bar{i}) \bar{Q}^{-1}(\bar{i}, \bar{i}') Q_T(\bar{i}', i), \end{aligned} \quad (37)$$

where

$$\alpha_T(j, i) = \alpha(j, i) + \sum_a \sum_{a'} A_r(j, a) Q^{-1}(a, a') C_{cap}(a', i). \quad (38)$$

When only the direct recombination coefficient $\alpha(j, i)$ is included in $\alpha_T(j, i)$, the first two terms in equation (37) correspond to the generalized collisional-radiative recombination coefficient recently defined by Burgess and Summers.⁸ The last term, which describes recombination from highly-excited levels \bar{i} produced by collisional excitation, will not usually be important. The definition of the collisional-dielectronic recombination coefficient between ground states which was introduced in the earlier paper by Burgess and Summers⁴ can be recovered by neglecting transitions between the autoionizing levels a .

The general expression obtained for the effective ionization coefficient is

$$S_{eff}(j, k) = S_T(j, k) - \sum_j \sum_{\bar{j}} Q(j, \bar{j}) \bar{Q}^{-1}(\bar{j}, \bar{j}') S_T(\bar{j}', k) - \sum_{\bar{k}} \sum_{\bar{k}'} S(j, \bar{k}) \bar{Q}^{-1}(\bar{k}, \bar{k}') Q_T(\bar{k}', k), \quad (39)$$

where

$$S_T(j, k) = S(j, k) + \sum_b \sum_{b'} A_a(j, b) Q^{-1}(b, b') C_e(b', k). \quad (40)$$

This effective ionization rate coefficient did not appear in previously reported statistical theories, because of the inherent restriction to only two consecutive ionization stages. Goldberg, Dupree, and Allen¹⁵ have found that the contributions from autoionization following inner-shell collisional excitation, which are represented by the second term in equation (40), can be comparable to the direct ionization coefficient $S(j, k)$.

At very low densities where practically all excited states decay by spontaneous radiative or autoionization processes in times that are short compared with their collision times, all ionization and recombination processes can be assumed to originate from the ground states. If the ground states of the three consecutive ionization stages are denoted by i_o , j_o , and k_o , the effective recombination and ionization coefficients $\alpha_{eff}(j_o, i_o)$ and $S_{eff}(j_o, k_o)$ which are obtained from the general expressions are found to reduce to the anticipated corona model definitions

$$\alpha_c(z+1 \rightarrow z) = \sum_j \left[\alpha(j, i_o) + \sum_a \frac{A_r(j, a) C_{cap}(a, i_o)}{A_a(a) + A_r(a)} \right] \quad (41)$$

and

$$S_c(z-1 \rightarrow z) = \sum_j \left[S(j, k_o) + \sum_b \frac{A_a(j, b) C_e(b, k_o)}{A_a(b) + A_r(b)} \right], \quad (42)$$

in which the sum over j now includes all bound states of the z -times ionized ion.

If use is made of the identities

$$1 - \sum_j \frac{A_a(j, b)}{A_a(b) + A_r(b)} = \sum_k \frac{A_r(k, b)}{A_a(b) + A_r(b)} \quad (43)$$

and

$$1 - \sum_j \frac{A_r(j, a)}{A_a(a) + A_r(a)} = \sum_i \frac{A_a(i, a)}{A_a(a) + A_r(a)}, \quad (44)$$

the effective loss rate $Q_{eff}(j_o, j_o)$ obtained from the general expression can be reduced to the simple result

$$Q_{eff}(j_o, j_o) = N_e [\alpha_c (z \rightarrow z - 1) + S_c (z \rightarrow z + 1)], \quad (45)$$

which is the sum of the corona model recombination and ionization rates defined by analogy with equations (41) and (42).

We have demonstrated that, in the corona model approximation, the recombination and ionization rates which appear in the total loss rate are defined in the same manner as the production rates arising from transitions originating from the two neighboring ionization stages. If the ground state population densities are now denoted simply by $N(z)$, the time-dependent equations simplify to the familiar corona model relationships

$$\begin{aligned} \frac{dN(z)}{dt} = & - [\alpha_c (z \rightarrow z - 1) + S_c (z \rightarrow z + 1)] N(z) N_e \\ & + \alpha_c (z + 1 \rightarrow z) N(z + 1) N_e + S_c (z - 1 \rightarrow z) N(z - 1) N_e. \end{aligned} \quad (46)$$

The requirement that $\sum_z dN(z)/dt = 0$, which expresses the conservation of ions under the assumption that the excited levels have negligible populations compared with the ground levels, is most naturally satisfied if equation (45) is valid.

If the assumption is now made that only recombinations can produce highly-excited states which can be appreciably depopulated by collisional processes, the effective ionization

rate coefficient $S_{eff}(j_0, k_0)$ is still given by equation (42). However, the effective recombination rate coefficient $\alpha_{eff}(j_0, i_0)$ is now given by the collisional-dielectronic recombination coefficient defined by

$$\alpha_{cd}(z+1 \rightarrow z) = \alpha_T(j_0, i_0) - \sum_{\bar{j} \neq j_0} \sum_{\bar{j}' \neq j_0} Q(j_0, \bar{j}) \bar{Q}^{-1}(\bar{j}, \bar{j}') \alpha_T(\bar{j}', i_0), \quad (47)$$

where the coefficients $\alpha_T(j, i_0)$ for recombination into the levels j are defined by equation (38).

The simplification of the general expression for the effective loss rate $Q_{eff}(j_0, j_0)$ is now much more tedious. We anticipate that the contributions representing ionization of the highly-excited states \bar{k} populated by recombination can be combined with the corona recombination terms to yield the collisional-dielectronic recombination coefficient $\alpha_{cd}(z \rightarrow z-1) = \alpha_{cd}(k_0, j_0)$, which is defined by an expression analogous to equation (47). This simplification can be accomplished by utilizing the identities

$$\begin{aligned} 1 &= \sum_b \sum_j A_a(j, b) Q^{-1}(b, b') \\ &= \sum_b \sum_k A_r(k, b) Q^{-1}(b, b') \end{aligned} \quad (48)$$

and

$$\begin{aligned} 1 &= \sum_{\bar{k} \neq k_0} N_e S(j_0, \bar{k}) \bar{Q}^{-1}(\bar{k}, \bar{k}') \\ &= - \sum_{\bar{k} \neq k_0} Q(k_0, \bar{k}) \bar{Q}^{-1}(\bar{k}, \bar{k}'). \end{aligned} \quad (49)$$

The effective loss rate $Q_{eff}(j_0, j_0)$ is then found to be the sum of the corona model ionization rate $N_e S_c(z \rightarrow z+1)$ and the collisional-dielectronic recombination rate $N_e \alpha_{cd}(z \rightarrow z-1)$. The ground state population densities now satisfy the equations obtained from (46) after replacing both corona model recombination coefficients with the corresponding collisional-dielectronic recombination coefficients. In the following section, our calculations will be

described for the collisional-dielectronic recombination coefficient defined by equation (47).

IV. CALCULATIONS

In this section we describe the details and present some results of our calculations for the excited level populations and the collisional-dielectronic recombination rates of multiply-charged *Fe* ions. The present calculations represent an extension of our previously reported corona model calculations¹¹ to the intermediate density region, where the low-lying level populations are still close to their corona equilibrium values but the highly-excited levels important in dielectronic recombination are depopulated by both collisional and radiative processes.

We first consider the populations of the doubly-excited autoionizing levels specified by $a = i', nl$. Since inner-shell collisional excitation can be neglected for large n values, we can assume that these levels are populated predominantly by the radiationless capture process (19). The radiation less capture rate coefficient $C_{cap}(i \rightarrow a)$ can be expressed in terms of the rate $A_a(a \rightarrow i)$ for the inverse autoionization process by means of the detailed balance relationship

$$C_{cap}(i \rightarrow a) = 2^3 a_0^3 \pi^{3/2} \frac{g(a)}{2g(i)} (E_H/k_B T_e)^{3/2} \times \exp\left[\frac{E(i) - E(a)}{k_B T_e}\right] A_a(a \rightarrow i). \quad (50)$$

The statistical weights associated with the energy levels $E(i)$ and $E(a)$ are denoted by $g(i)$ and $g(a)$, respectively, and $E_H = 13.6$ eV. The other symbols have their conventional meaning.

For large values of n and z the autoionization rates $A_a(a \rightarrow i)$ can be obtained by using the quantum defect theory relationship derived by Seaton¹³, which may be expressed in the form

$$A_a(a \rightarrow i) = \frac{E_H}{\pi} \frac{2(z+1)^2}{\pi^2 n^3 a_0^2} \frac{g(i)}{g(a)} \left[\frac{E(i') - E(i)}{E_H} \right] \times \sum_{l_i} \sigma(i, \epsilon_i, l_i \rightarrow i', \epsilon_i', l_i')|_{\epsilon_i' \rightarrow 0}, \quad (51)$$

where $\sigma(i, \epsilon_i, l_i \rightarrow i', \epsilon_i', l_i')|_{\epsilon_i' \rightarrow 0}$ denotes the threshold value of the partial wave cross section for the electron impact excitation $i \rightarrow i'$ of the $(z+1)$ -times ionized ion. The electron impact excitation cross sections used in our calculations have been obtained by the distorted wave method described by Davis, Kepple, and Blaha¹⁶.

The decay rate for the stabilizing radiative transition (22) is obtained by making the customary approximation

$$A_r(a \rightarrow \bar{j}) = A_r(i' \rightarrow i_0), \quad (52)$$

in which the influence of the outer n -electron is neglected.

The autoionization processes and stabilizing radiative transitions which are taken into account in the present calculations are associated with single-electron electric-dipole de-excitations $i' \rightarrow i$ of the recombining ion. The radiative decay rates corresponding to a $\Delta n_i \neq 0$ transition increase as z^4 with increasing z . However, the dielectronic recombination of the $Fe^{+8} - Fe^{+13}$ ions is accomplished primarily through $3d \rightarrow 3p$ transitions, for which the radiative decay rates increase only linearly with z . Consequently, the stabilizing radiative decay process becomes competitive with autoionization only for relatively large values of the outer electron principal quantum number ($n \sim 100$). Finally, we note that the $3d \rightarrow 3p$ collisional stabilization rate becomes comparable to $A_r(3d \rightarrow 3p)$ only at $N_e = 10^{19} \text{ cm}^{-3}$. Equation (23) is, therefore, valid for the density range considered in this investigation.

The rate coefficient describing collisionally-induced angular momentum mixing of the outer n -electron state is given in the Bethe-approximation by

$$\begin{aligned}
C_{z_0}(nl \rightarrow n, l \pm 1) &= \left(\frac{\mu}{m_e} \right)^{1/2} z_0^2 \left(\frac{32\pi^{3/2}}{\sqrt{3}} \right) \left(\frac{a_0^3 E_H}{\pi} \right) \\
&\times \left(\frac{3}{4} \right) \left(\frac{l_{>}}{2l+1} \right) \left(\frac{n}{z+1} \right)^2 (n^2 - l_{>}^2) \\
&\times \left(\frac{E_H}{k_B T} \right)^{1/2} \frac{\sqrt{3}}{2\pi} E_1(y),
\end{aligned} \tag{53}$$

where

$$y = \left[\frac{n^2}{2(z+1)E_H} \right]^2 \left(\frac{\mu}{m_e} \right) \left(\frac{E_H}{k_B T} \right) (\Delta E_l^2 + \Gamma_l^2 + \hbar^2 \omega_p^2). \tag{54}$$

The charges on the projectile and target particles are denoted by z_0 and z , respectively, and μ is the reduced mass. The argument y of the exponential integral E_1 is made finite, as suggested by Griem¹⁷, by taking into account the plasma frequency ω_p , the l -sublevel energy separation ΔE_l , and the width Γ_l due to the finite natural lifetime. A similar result obtained by Pengelly and Seaton¹⁸ does not include the l -sublevel separation, which can be important in a multiply-charged ion. In our calculations, the l -sublevel separations were estimated by taking into account the long-range monopole-quadrupole interactions and the fine structure splittings.

The normalized population densities $\rho(a) = N(a)/N(i_0)N_e$ of the doubly-excited levels $a = i', nl$, which are formed by radiationless capture from the ground state i_0 , are given by

$$\rho(a) = \sum_{a'} Q^{-1}(a, a') C_{cap}(a', i_0). \tag{55}$$

With account taken of the angular momentum redistribution processes (9) and (10), the non-zero elements of the matrix Q are given by

$$\begin{aligned}
-Q(a, a') &= W(a, a') = N_e C_e(nl' \rightarrow nl) \\
&+ N_{H+} C_{H+}(nl' \rightarrow nl)
\end{aligned} \tag{56}$$

and

$$Q(a, a) = A_a(a) + A_r(a) + \sum_{a' \neq a} W(a', a), \quad (57)$$

where a' differs from a only in the outer electron angular momentum quantum number $l' = l \pm 1$. The sum over a' in equation (55) is actually a sum over all $l' = 0, n - 1$. The rate coefficient describing the production of the singly-excited bound states $\bar{j} = i_0, nl$ by dielectronic recombination, which corresponds to the second term in equation (38), is expressed in terms of the normalized doubly-excited level population densities $\rho(a)$ by

$$\alpha_d(\bar{j}, i_0) = \sum_a A_r(\bar{j}, a) \rho(a). \quad (58)$$

Because of the approximation given by equation (52) for $A_r(a \rightarrow \bar{j})$, the sum over a is actually a sum only over the different excited states i' .

In our previous investigation⁶, the effects of angular momentum redistribution due to protons were included by using the quasi-static and linear Stark effect approximations. The treatment in terms of proton impacts adopted here, which is essentially the same as that of Seaton and Storey⁷, is expected to predict less angular momentum redistribution for a given value of n . When it becomes necessary to account for the angular momentum redistribution produced by other impurity ions, the quasi-static may be the more appropriate of the two extreme approximations.

With increasing n , the autoionization rate decreases as n^{-3} whereas the rate for collisionally induced angular momentum mixing increases as n^4 . However, the radiative decay rate given by equation (52) is independent of n . Consequently, the collisional processes are expected to be capable of establishing a Boltzmann distribution with respect to l only for much higher values of n than in the case of the singly-excited bound states, for which the radiative decay rates decrease as n^{-3} . Accordingly, the less rapid collisional processes connecting doubly-excited levels associated with different n -values can probably be neglected.

The effects of collisionally-induced angular momentum redistribution are illustrated for three different densities in Figures 2 and 3, in which the coefficients obtained from equation (58) for the dielectronic recombination of Fe^{+10} are shown as functions of l for $n = 20$ and 30, respectively. Both the electron and the proton temperatures were taken to equal to 100 eV, which is close to the maximum abundance temperature predicted by our previously reported corona equilibrium calculations¹¹. The results obtained at $N_e = 10^{10} \text{ cm}^{-3}$ are indistinguishable from the values predicted without the inclusion of angular momentum redistribution. For $n = 30$ (Figure 3), the results obtained at $N_e = 10^{16} \text{ cm}^{-3}$ are close to the limiting values predicted on the basis of a Boltzmann distribution with respect to l . Results similar to those presented in Figures 2 and 3 have been obtained for C^+ by Seaton and Storey⁷.

The coefficients for the dielectronic recombination of Fe^{+10} obtained from equation (58) after summation with respect to l are shown as functions of n in Figure 4. As anticipated, angular momentum redistribution is found to become more effective with increasing N_e and n . The amplification in the dielectronic recombination coefficients can be directly attributed to an increase in the populations of the higher- l doubly-excited levels, which have larger statistical weights and practically zero probabilities of formation directly through radiationless capture and decay through autoionization. The rate of photon emission through stabilizing radiative transitions, which is obtained after summation with respect to n , is found to be enhanced by about a factor of 3 over the low-density result by a density of 10^{16} cm^{-3} . This effect may be observable in the emission spectrum near the resonance line of the recombining ion.

We now consider the populations of the singly-excited bound levels $\bar{j} = i_o, nl$ produced by recombinations. According to equation (38), the total recombination coefficient $\alpha_T(\bar{j}, i_o)$ into level \bar{j} is the sum of the total direct recombination coefficient $\alpha(\bar{j}, i_o)$ and the dielectronic recombination coefficient $\alpha_d(\bar{j}, i_o)$ defined by equation (58). The total direct recombination

coefficient is obtained from the direct radiative recombination coefficient and the three-body recombination coefficient by means of equation (16). The direct radiative recombination coefficient $\alpha_r(i_o \rightarrow \bar{j})$ can be estimated by using the expression presented in our previous paper¹¹, which takes into account the presence of N_i equivalent electrons in the outermost $n_i l_i$ subshell of the recombining ion. The three-body recombination coefficient $\alpha_3(i_o \rightarrow \bar{j})$ is obtained from the electron impact ionization coefficient $S_e(\bar{j} \rightarrow i_o)$ by means of a detailed balance relationship analogous to equation (50).

The electron impact ionization rate coefficient obtained in the Bethe and unit-Gaunt-factor approximations may be written as

$$\begin{aligned}
 S_e(j \rightarrow i_o) &= \frac{2^8 \pi^{-1/2}}{3\sqrt{3}} \left(\frac{a_o^3 E_H}{\pi} \right) \frac{1}{(2l+1)} \\
 &\times \frac{(z+1)^4}{n^3} [1 + \delta(nl, n_i l_i) N_i] (E_H/k_B T_e)^{1/2} \\
 &\times \left\{ (E_H/y k_B T_e)^3 \left[\frac{1}{3} E_1(y) + \left(\frac{1}{3} \ln 4 - \frac{1}{9} \right) \exp(-y) \right] \right. \\
 &\quad - (E_H/k_B T_e)^3 \left[\frac{1}{3} \ln 4 - \frac{1}{9} \right] \left[\frac{1}{2} y^{-2} \exp(-y) \right. \\
 &\quad \left. \left. - \frac{1}{2} y^{-1} \exp(-y) + \frac{1}{2} E_1(y) \right] \right\}, \quad (59)
 \end{aligned}$$

where

$$y = [E(i_o) - E(j)]/k_B T_e. \quad (60)$$

The accuracy of this expression is expected to improve with increasing n .

The relative importance of dielectronic recombination, direct radiative recombination, and three-body recombination is illustrated in Figure 5 by showing the individual contributions to $\sum_i \alpha_T(\bar{j}, i_o)$ as functions of n for the recombination of Fe^{+10} at $T_e = 100$ eV and $N_e = 10^{16} \text{ cm}^{-3}$.

Direct radiative recombination can be seen to be negligible, while three-body recombination prevails over dielectronic recombination only for $n > 40$.

In order to obtain the population densities of the singly-excited levels, it will be necessary to estimate the bound-bound transition rates which enter into the construction of the matrix \bar{Q} . The rate coefficient describing $\Delta n \neq 0$ electron impact excitations is given in the Bethe approximation by

$$C_e(nl \rightarrow n', l' = l \pm 1) = \left[\frac{32\pi^{3/2}}{\sqrt{3}} \right] \left[\frac{a_0^3 E_H}{\pi} \right] \times f(nl \rightarrow n' l') \frac{1}{y} \exp(-y) (E_H/k_B T_e)^{3/2} \times \frac{\sqrt{3}}{2\pi} [\ln 4 + \exp(y) E_1(y)], \quad (61)$$

where

$$y = [E(n' l') - E(nl)]/k_B T_e \quad (62)$$

and $f(nl \rightarrow n' l')$ is the oscillator strength for the dipole transition which is approximated in our calculations by using the hydrogenic value. The de-excitation rate is obtained from the excitation rate by means of a detailed balance relationship. $n \rightarrow n \pm 1$ transitions are found to be the most rapid $\Delta n \neq 0$ collisional processes. For the n -levels considered, the $n \rightarrow n+1$ excitation processes are found to be more probable than the direct ionization process.

In previously reported calculations for the collisional-dielectronic recombination coefficients^{4,7}, it has been assumed that the collisional processes are rapid enough to establish a Boltzmann distribution of the singly-excited bound level populations with respect to l for all values of n . This assumption becomes questionable in multiply-charged ions, where the fine-structure splitting of the l -sublevels scales as z^4 . In this investigation, we take into account the

rates for collisionally-induced angular momentum mixing of the singly-excited bound states \bar{j} by using equation (54) for both protons and electrons.

The radiative decay rates $A_r(nl \rightarrow n', l \pm 1)$ are approximated by using the hydrogenic values.

The normalized population densities $\rho(\bar{j}) = N(\bar{j})/N(i_0)N_e$ of the singly-excited bound levels $\bar{j} = i_0, nl$, produced by recombinations from the ground state i_0 , are given by

$$\rho(\bar{j}) = \sum_{\bar{j}'=i_0, n'l'} \bar{Q}^{-1}(\bar{j}, \bar{j}') \alpha_T(\bar{j}', i_0). \quad (63)$$

The matrix elements of \bar{Q} are given by

$$\begin{aligned} -\bar{Q}(\bar{j}, \bar{j}') &= W(\bar{j}, \bar{j}') \\ &= N_e C_e(n' l' \rightarrow nl) + N_{H^+} C_{H^+}(n' l' \rightarrow nl) \delta(n', n) \\ &\quad + A_r(n' l' \rightarrow nl) \theta[E(n' l') - E(nl)] \text{ for } \bar{j} \neq \bar{j}' \end{aligned} \quad (64)$$

and

$$\bar{Q}(\bar{j}, \bar{j}) = N_e S_e(\bar{j} \rightarrow i_0) + \sum_{\bar{j} \neq j} W(\bar{j}, \bar{j}). \quad (65)$$

The collisional-dielectronic recombination coefficient is given, in terms of the normalized singly-excited bound level population densities $\rho(\bar{j})$, by

$$\begin{aligned} \alpha_{cd}(j_0, i_0) &= \alpha_T(j_0, i_0) \\ &\quad + \sum_{\bar{j} \neq j_0} W(j_0, \bar{j}) \rho(\bar{j}). \end{aligned} \quad (66)$$

With increasing n , collisional processes will tend to bring the singly-excited level population densities closer to their Boltzmann-Saha equilibrium values. Accordingly, it is customary to express the normalized population densities $\rho(\bar{j})$ in terms of the departure coefficients $b(nl)$, defined by

$$\rho(\bar{j}) = 2^3 a_0^3 \pi^{3/2} (E_H/k_B T_e)^{3/2} \times \exp \left[\frac{E(i_0) - E(\bar{j})}{k_B T_e} \right] (2l + 1) b(nl), \quad (67)$$

which approach unity for sufficiently large n . The matrix \bar{Q} must, therefore, be constructed only within the subspace of the nl -levels for which $b(nl)$ differs substantially from unity. Since direct inversion of this matrix is still impractical for the large n -values of importance, we have adopted the matrix condensation and Lagrangian interpolation techniques developed by Burgess and Summers^{4,8} in order to reduce the matrix to a manageable size. Briefly, a representative set of nl levels is selected, and the complete set of level population densities is expressed in terms of the representative values by means of the appropriate Lagrangian interpolation coefficients. Because of the necessity to interpolate with respect to both n and l , the present interpolation scheme is greatly increased in complexity in comparison with the one used by Burgess and Summers^{4,8}, who assumed that the l -sublevels have relative populations given by the Boltzmann distribution for all values of n .

The departure coefficients $b(nl)$ for recombination onto Fe^{+9} are shown in Figure 6 as functions of l for $n = 10, 20$, and 30 at $N_e = 10^{14}$ and 10^{16} cm^{-3} . The characteristic overpopulation of the nl -levels which is produced by dielectronic recombination can be clearly seen. The assumption that a Boltzmann distribution with respect to l is established for all n -values, which is inherent in all previously reported calculations of α_{cd} , is found to be questionable. The departure coefficients for $l = 0$, which are illustrated as functions of n in Figure 7, show that the approach to Boltzmann-Saha equilibrium with increasing N_e and n can be rather slow.

The collisional-dielectronic recombination coefficient for the recombination of Fe^{+10} is shown in Figure 8 as functions of temperature for three different densities. The results obtained for $N_e = 10^{10} \text{ cm}^{-3}$ are essentially the same as our previously reported¹¹ corona model values, while the results obtained for $N_e = 10^{16} \text{ cm}^{-3}$ are found to be reduced from the coro-

na model values by about an order of magnitude due to the effects of collisional processes on the highly-excited bound levels of the recombined ion. A similar figure has been presented for Fe^{+8} by Burgess and Summers⁴.

The collisional-dielectronic recombination rate coefficients obtained for the recombination of $Fe^{+8} - Fe^{+13}$ at $N_e = 10^{16} \text{ cm}^{-3}$, which are tabulated in Table 1 as functions of temperature, are found to be reduced from their corona model values by at least an order of magnitude. Recently¹⁹, the effective rate coefficients for the recombination of $Fe^{+9} - Fe^{+11}$ have been deduced experimentally by analyzing the time-dependent line emission spectra produced by iron ions injected into a theta-pinch plasma with an electron density slightly greater than 10^{16} cm^{-3} . Their preliminary analysis, based on a time-dependent corona ionization-recombination model, indicates that the effective recombination rate coefficients are indeed lower than predicted by our corona model calculations¹¹.

V. CONCLUSIONS

In this investigation we have generalized previously reported statistical theories to obtain the contributions from highly-excited bound and autoionizing levels to effective transition rates between the low-lying bound levels in three consecutive ionization stages. We have also demonstrated that the familiar corona model equations can be recovered at very low-densities. At densities for which only the highly-excited levels involved in dielectronic recombination are appreciably depopulated by collisional processes, the effective ionization rate is practically unaltered but the effective recombination rate can be substantially reduced. Calculations have been carried out for the excited level populations and the collisional-dielectronic recombination coefficients of $Fe^{+8} - Fe^{+13}$ ions, which recombine through very large values of the outer electron principal quantum number. To the best of our knowledge, the present calculations are the first in which explicit account has been taken of the transition rates for collisionally-

induced angular momentum mixing of both the singly-excited bound states and the doubly-excited autoionizing states. In a future investigation, more extensive results for collisional-dielectronics recombination coefficients will be presented together with new results for the ionization equilibrium and the radiative energy loss rates for various low- and high-Z elements.

ACKNOWLEDGMENTS

The authors are indebted to H.R. Griem and R.L. Brooks for detecting an error in a preliminary version of the manuscript and for numerous helpful and stimulating discussions relating to their experimental investigation.

This work has been supported by the E.O. Hulbert Center for Space Research, Naval Research Laboratory, as part of the Apollo Telescope mount Data Analysis Program funded by the National Aeronautics and Space Administration under Grant No. DPR-60404-G and by the Office of Naval Research.

REFERENCES

1. H.R. Griem, *Plasma Spectroscopy*, (McGraw-Hill, New York, 1964).
2. A.H. Gabriel and C. Jordan, in *Case Studies in Atomic Collision Physics II*, edited by E.W. McDaniel and M.R.C. McDowell (North-Holland, Amsterdam, 1972), Chap. 4.
3. A. Burgess, *Astrophys. J.* **139**, 776 (1964).
4. A. Burgess and H.P. Summers, *Astrophys. J.* **157**, 1007 (1969).
5. D.R. Bates, A.E. Kingston, and R.W.P. McWhirter, *Proc. Roy. Soc. London, Ser. A* **267**, 297 (1962).
6. V.L. Jacobs, J. Davis, and P.C. Kepple, *Phys. Rev. Letters* **37**, 1390 (1976).
7. M.J. Seaton and P.J. Storey, in *Atomic Processes and Applications*, edited by P.G. Burke and B.L. Moiseiwitsch (North-Holland, Amsterdam, 1976), Chap. 6.

8. A. Burgess and H.P. Summers, *Mon. Not. Roy. Astron. Soc.*, **174**, 345 (1976).
9. J.C. Weisheit, *J. Phys. B*, **8**, 2556 (1975).
10. T. Åberg, *Phys. Rev. A*, **4**, 1735 (1971).
11. V.L. Jacobs, J. Davis, P.C. Kepple, and M. Blaha, *Astrophys. J.* **211**, 605 (1977).
12. D.R. Bates and A. Dalgarno, in *Atomic and Molecular Processes*, edited by D.R. Bates (Academic Press, New York and London, 1962), p. 245.
13. M.J. Seaton, *J. Phys. B*, **2**, 5 (1969).
14. B.W. Shore, *Astrophys. J.* **158**, 1205 (1969).
15. L. Goldberg, A.K. Dupree, and J.W. Allen, *Ann d'Ap.*, **28**, 589 (1965).
16. J. Davis, P.C. Kepple, and M. Blaha, *J. Quant. Spectrosc. Radiat. Transfer* **16**, 1043 (1976).
17. H.R. Griem, private communication.
18. R.M. Pengelly and M.J. Seaton, *Mon. Not. Roy. Astron. Soc.*, **127**, 165 (1964).
19. R.L. Brooks, R.U. Datta, and H.R. Griem, private communication.

Table 1 — α_{cd} ($\text{cm}^3 \text{ sec}^{-1}$), $N_e = 10^{16} \text{ cm}^{-3}$.

$\log_{10} T_e (\text{eV})$	Fe^{+8}	Fe^{+9}	Fe^{+10}	Fe^{+11}	Fe^{+12}	Fe^{+13}
1.6	0.51(-10)	0.48(-10)	0.47(-10)	0.10(-9)	0.11(-9)	0.13(-9)
1.8	0.28(-10)	0.21(-10)	0.27(-10)	0.51(-10)	0.40(-10)	0.27(-10)
2.0	0.11(-10)	0.16(-10)	0.17(-10)	0.24(-10)	0.18(-10)	0.13(-10)
2.2	0.12(-10)	0.97(-11)	0.89(-11)	0.91(-11)	0.75(-11)	0.67(-11)
2.4	0.21(-10)	0.63(-11)	0.54(-11)	0.53(-11)	0.41(-11)	0.29(-11)
2.6	0.22(-11)	0.17(-11)	0.18(-11)	0.34(-11)	0.24(-11)	0.17(-11)
2.8	0.17(-11)	0.12(-11)	0.12(-11)	0.15(-11)	0.13(-11)	0.11(-11)
3.0	0.14(-11)	0.72(-12)	0.71(-12)	0.92(-12)	0.78(-12)	0.62(-12)

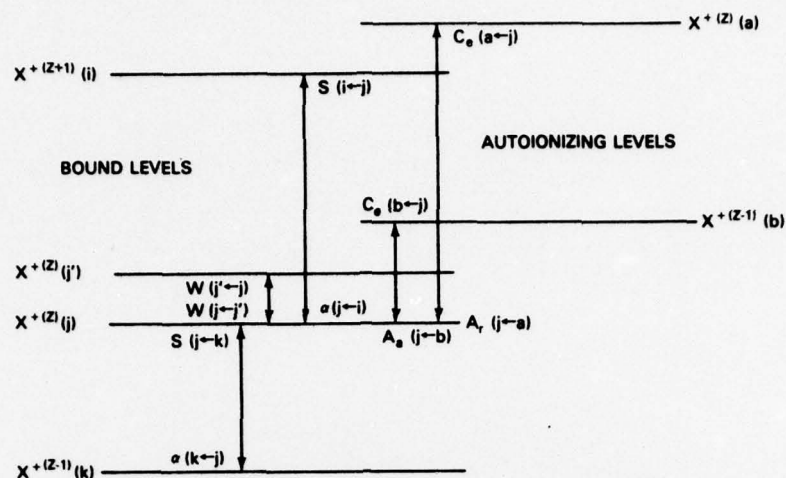


Fig. 1 - The transitions, involving bound and autoionizing levels in three consecutive ionization stages, which are taken into account in the determination of the bound level populations $N(i)$ of $X^{+(z)}$. As described in the text, some of the rates and rate coefficients include contributions from both collisional and radiative processes.

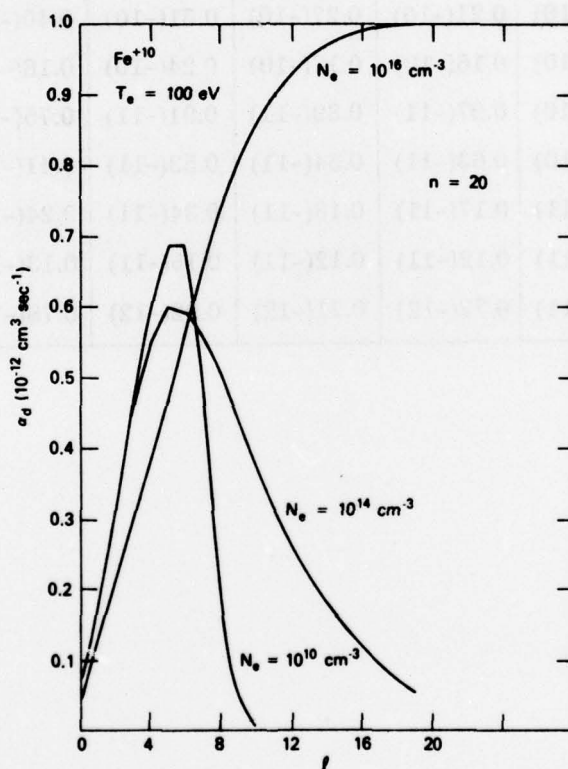


Fig. 2 - The rate coefficients for the dielectronic recombination of Fe^{+10} into the nl -levels of Fe^{+9} corresponding to $n = 20$.

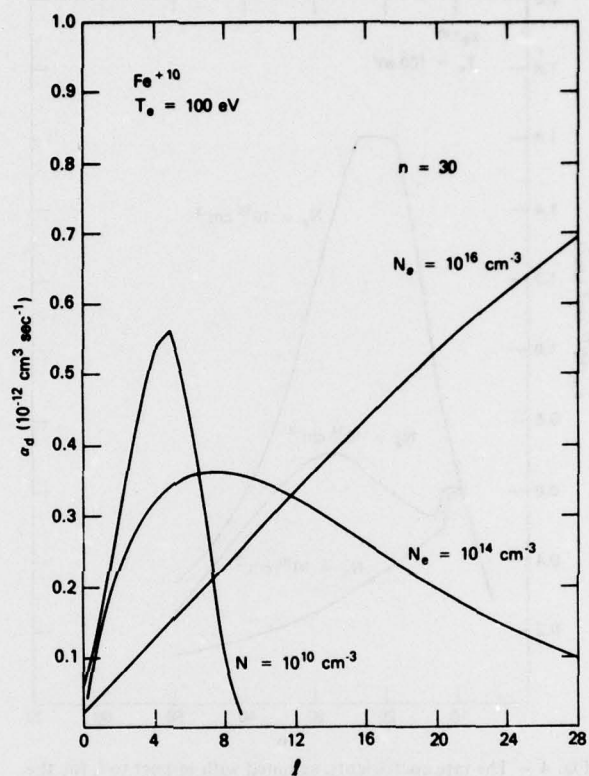


Fig. 3 – The rate coefficients for the dielectronic recombination of Fe⁺¹⁰ into the *nl*-levels of Fe⁺⁹ corresponding to *n* = 30.

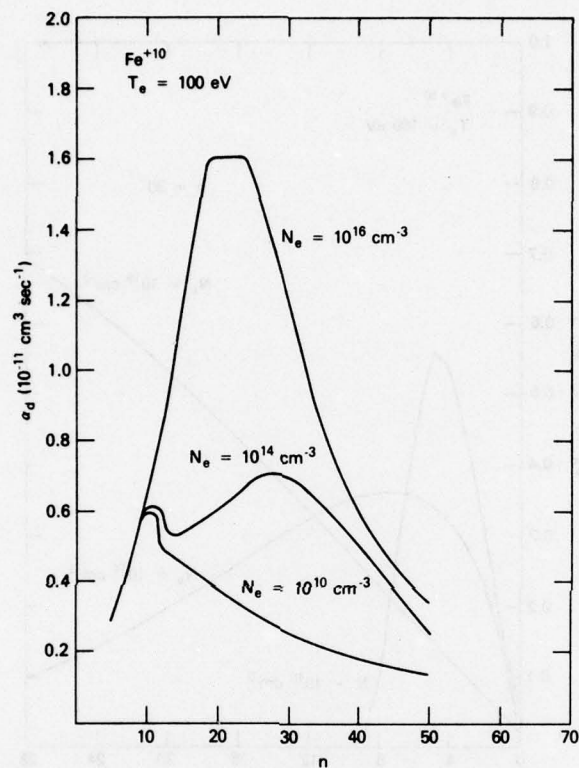


Fig. 4 - The rate coefficients, summed with respect to l , for the dielectronic recombination of Fe^{+10} into the nl -levels of Fe^{+9} .

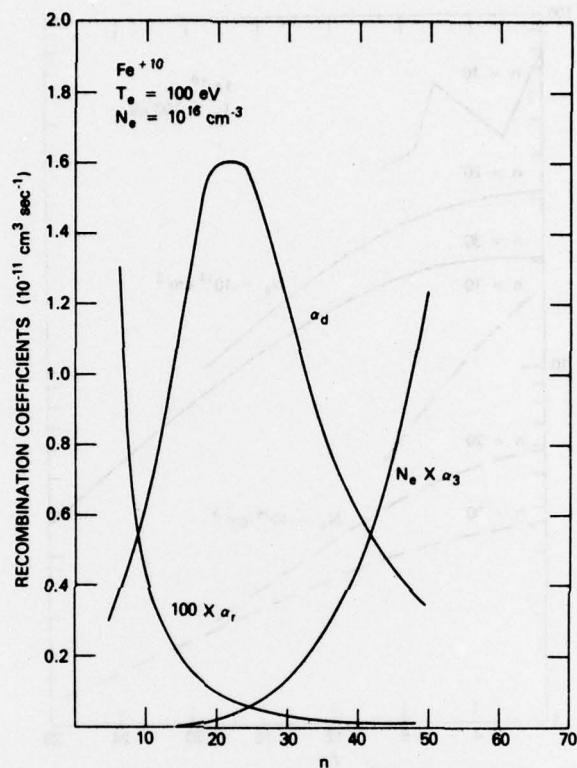


Fig. 5 — The rate coefficients, summed with respect to l , describing the production of the nl -levels of Fe^{+9} by dielectronic recombination (α_d), direct radiative recombination (α_r), and three-body recombination ($N_e \times \alpha_3$).

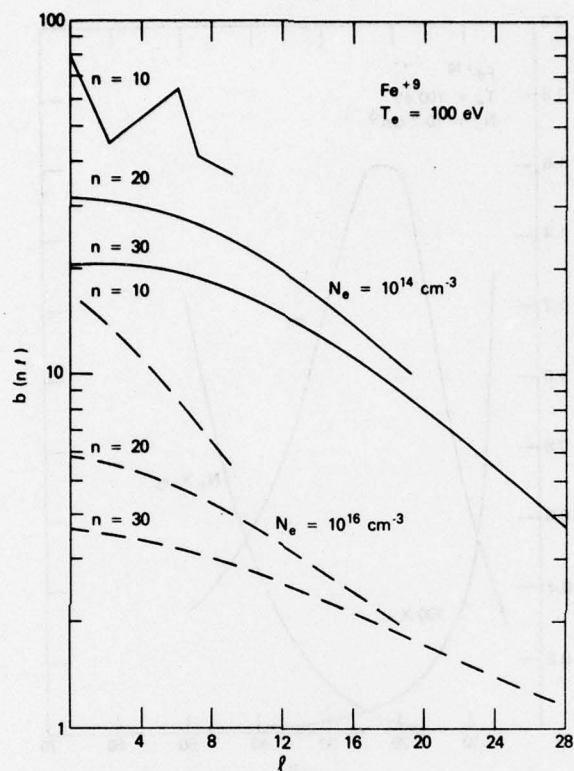


Fig. 6 - The departure coefficients $b(nl)$ for recombination into representative nl -levels of Fe^{+9} .

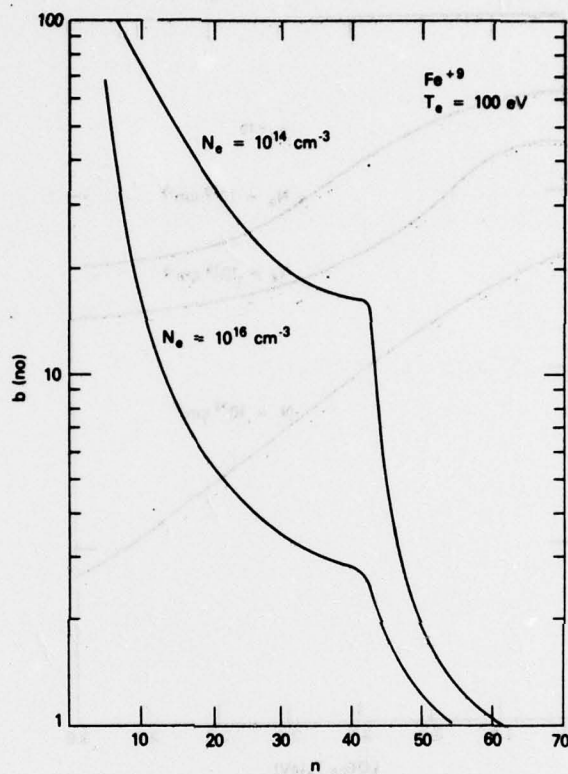


Fig. 7 - The departure coefficients $b(nl)$, corresponding to $l = 0$, for recombination into the nl -levels of Fe^{+9} .

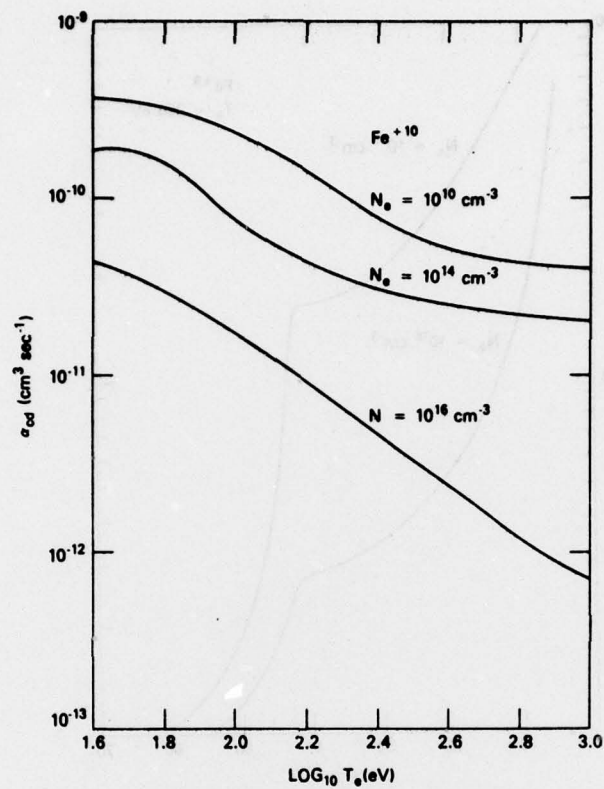


Fig. 8 - The collisional-dielectronic recombination coefficient for the recombination of Fe^{+10} .